Analysis of turbine-grid interaction of grid-connected wind turbine using HHT

A Chen[1], W Wu[1], J Miao[1] and D Xie[1]

[1] Department of Electronic Information and Electrical Engineering, Shanghai Jiao Tong University, 800 Dongchuan Road, Shanghai, China

Abstract. This paper processes the output power of the grid-connected wind turbine with the denoising and extracting method based on Hilbert Huang transform (HHT) to discuss the turbine-grid interaction. At first, the detailed Empirical Mode Decomposition (EMD) and the Hilbert Transform (HT) are introduced. Then, on the premise of decomposing the output power of the grid-connected wind turbine into a series of Intrinsic Mode Functions (IMFs), energy ratio and power volatility are calculated to detect the unessential components. Meanwhile, combined with vibration function of turbine-grid interaction, data fitting of instantaneous amplitude and phase of each IMF is implemented to extract characteristic parameters of different interactions. Finally, utilizing measured data of actual parallel-operated wind turbines in China, this work accurately obtains the characteristic parameters of turbine-grid interaction of grid-connected wind turbine.

1. Introduction

Currently, with the increasing permeability of wind power in power grid, more and more remarkable environmental and economic benefits are achieved. However, problems of power-quality caused by grid-connected wind turbines should not be ignored [1]. Due to the interactions in components of electrical coupling and mechanical connection between wind turbines and power grid, output waveforms of wind turbines contain various kinds of vibration signals with different frequencies, which are referred to as turbine-grid interaction, during the grid-connected operations [2]. At present, turbine-grid interaction is commonly classified into two categories: sub-synchronous interaction (SSI) [3] and low-frequency oscillation (LFO) [4]. Then, SSI is divided into sub-synchronous control interaction (SSCI) and sub-synchronous torsional interaction (SSTI), which is composed of sub-synchronous resonance (SSR) and sub-synchronous oscillation (SSO). In figure 1, the relationship of them is clearly illustrated.
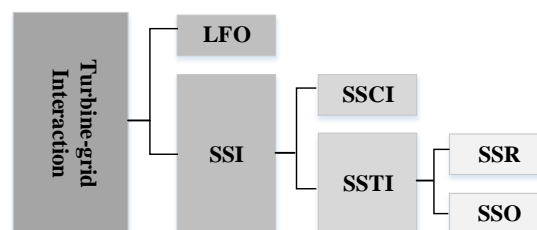

Figure 1. classification diagram of turbine-grid interaction

The turbine-grid interaction can result in reduced efficiency, increased life loss of wind turbines and rising failure rate of sensitive equipment, leading to sharp fall in productivity and influencing the security and stability of power grid operation [5], [6]. Aiming at the destructive effects of the turbine-gird

interactions on the normal operation of power grid, a plenty of studies focus on the methods to identify accurately the interactions implicit in the output waveforms of wind turbines, which lay a foundation for researches on corresponding countermeasures that can reduce operational and financial damage caused by turbine-grid interactions. The main methods are twofold. The first method is small signal analysis, whose weaknesses are the construction of complex small perturbation model and off-line application [7]. The other method is modern signal processing, including fast Fourier transform (FFT) [8], wavelet transform (WT) [9] and, recently, Hilbert Huang transform (HHT) [10].

Since HHT can adaptively decompose complicated waveforms with an excellent time resolution (the time at which frequencies change), it is suitable for analysing nonlinear and nonstationary data detected in power system. In [11], a filtering method based on HHT is proposed to extract low frequency oscillation in Western Japan 60-Hz power system. Authors of [12] present a modified HHT for time-frequency analysis of distorted power quality signals.

This paper exploits the potential of HHT to implement noise detection and reduction of output power of grid-connected wind turbines and extract characteristic parameters of turbine-grid interaction. The following structure is as follows: Section 2 introduce the principle of HHT, and the extraction flow is presented in section 3. In section 4, there is a case analysis. Lastly, conclusions are drawn in section 5.

2. HHT

Output waveforms of wind turbines are typically nonlinear and nonstationary signals, so that HHT is well suited for processing them. HHT consists of two steps: EMD and HT [12].

2.1. EMD

The essence of EMD is decomposing the original signal into a series of Intrinsic Mode Functions (IMFs), which is axial symmetry, and a residue, as shown in (1).

$$x(t) = \sum_{i=1}^{n} I_i(t) + r_n(t) \tag{1}$$

Where $x(t)$ is the original signal, $I_i(t)$ is the ith IMF, $r_n(t)$ is the residue that represents the average trend of the original signal.

Simultaneously, IMF must meet the succeeding conditions: 1) There is one zero crossing point between any adjacent local extreme point. 2) The local mean at any time is zero. Thus, the steps of EMD can be described as follows:

Step I   Employ spline interpolations to obtain maxima and minima envelopes ($E_{max}(t)$ and $E_{min(t)}$) of the original signal $x(t)$.

Step II   Calculate the candidate for the first IMF with the subsequent equation.

$$P_1 = x(t) - \left[E_{max}(t) + E_{min}(t) \right]/2 \tag{2}$$

Step III Judge whether $P_1(t)$ meets the aforementioned requirements to be an IMF. If yes, the first IMF $I_1(t) = P_1(t)$, if not, then, repeat Step I and II on the premise of regarding $P_1(t)$ as the original signal until $P_1(t)$ becomes an IMF.

Step IV   Calculate the first residue $r_1(t)$ and test whether the number of extreme point of $r_1(t)$ is less than or equal to one. If yes, terminate EMD, otherwise repeat Step I, II and III on $r_1(t)$.

2.2. HT

Once all the IMFs are extracted from the original signal, IMFs are processed by HT to obtain their instantaneous amplitudes and frequencies. The HT $\hat{I}(t)$ of the IMF signal $I(t)$ can be obtained as

$$\hat{I}(t) = H\left[I(t) \right] = \frac{1}{\pi} \int_{-\infty}^{+\infty} \frac{I(\tau)}{t - \tau} d\tau \tag{3}$$

So analytic signal of HT and its corresponding calculations are shown as follows.

$$Z(t) = I(t) + i\hat{I}(t) = a(t) \exp(i\theta(t)) \tag{4}$$

$$a(t) = \left[I(t)^2 + \hat{I}(t)^2 \right]^{1/2} \tag{5}$$

$$\theta(t) = \arctan\left[\hat{I}(t) / I(t) \right] \tag{6}$$

$$f(t) = \frac{1}{2\pi} \frac{d\theta(t)}{dt} \tag{7}$$

Where $Z(t)$ is analytic signal, $a(t)$ is instantaneous amplitude, $\theta(t)$ is instantaneous phase and $f(t)$ represents instantaneous frequency.

3. Processing methods

3.1. Signal denoising

For better analysis of original signal, the noise implicit in the signal should be eliminated. In this work, two indexes are employed to evaluate each IMF: energy ratio, the smaller it is, the less important the IMF is, and power volatility, the drastic change of which represents the huge role played by the IMF. IMFs which feature different amplitudes contain distinct amounts of energy, and energy of the ith IMF can be calculated as

$$W_i = \sum_{i=1}^{N} \left| a_i(t) \right|^2 \Big/ N \tag{8}$$

Where N is the total number of data points. Thus, energy ratio is defined as

$$R_i = W_i / W = W_i \Big/ \sum_{i=1}^{n} W_i \tag{9}$$

Where W is the sum of energy. Moreover, power volatility reflects the fluctuation level of output power of wind turbines. Hence, the volatility of each IMF, which has specific frequency, can be calculated by (10) and utilized to investigate the main frequencies of wind power fluctuation.

$$V(t) = \frac{\max\left[P_{local}(t) \right] - \min\left[P_{local}(t) \right]}{P_{rated}} \times 100\% \tag{10}$$

Where $V(t)$ is the power volatility, $\max\left[P_{local}(t) \right]$ is the maximum power in a certain period of time, $\min\left[P_{local}(t) \right]$ is the minimum power, and P_{rated} is the rated capacity of wind turbine.

Extraction of characteristic parameters of turbine-grid interactions

In power system, turbine-grid interaction can be expressed as

$$x(t) = Ae^{-\lambda t} \cos(wt + \theta_0) \tag{11}$$

Where A is the initial amplitude, λ is attenuation coefficient, w is frequency and θ_0 is initial phase. When HT is carried out on the turbine-gird interaction $x(t)$, combined with (4)~(6), (11) can be transformed to the following equations.

$$a(t) = \left[x(t)^2 + \hat{x}(t)^2 \right]^{1/2} = Ae^{-\lambda t} \Rightarrow \ln a(t) = -\lambda t + \ln A \tag{12}$$

$$\theta(t) = wt + \theta_0 \tag{13}$$

Subsequently, data fitting of instantaneous amplitude and phase of each IMF is performed to obtain accurate A, λ, w and θ_0. Then, damping ratio can be calculated as

$$\zeta = \lambda \Big/ \left[(w)^2 + (\lambda)^2 \right] \tag{14}$$

4. Cases analyses

To study the turbine-grid interaction between grid-connected wind power and power grid, measured data of actual parallel-operated wind turbine in China is used. Based on the above signal processing methods, the concrete analysis flow is shown in figure 2.
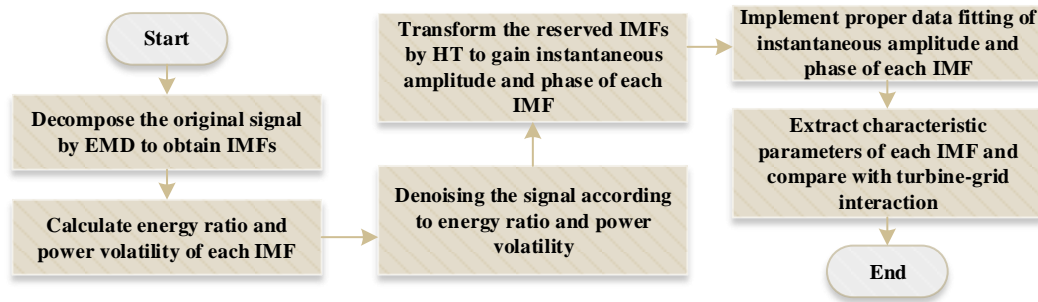
Figure 2. Analysis flow of measured data of wind turbines

The capacity of the wind turbine is 2 MW. The sampling frequency of data is 4000 Hz, and this paper takes a set of 40000 points, that is a group of 10 s data.

Firstly, the output power is decomposed into 13 IMFs and a residue, as shown in figure 3. Then we can gain instantaneous amplitude and phase and calculate the energy ratio and power volatility of each IMF, which can be clearly found in table 1 and figure 4. Obviously, energy ratios of IMF8~IMF13 is very small and power volatilities of IMF5~IMF13 keep basically stable, which mean that IMF8~IMF13 have small fluctuation and include little information of output power. Thus, the elimination of these components has slight impact on the analysis of the signal.
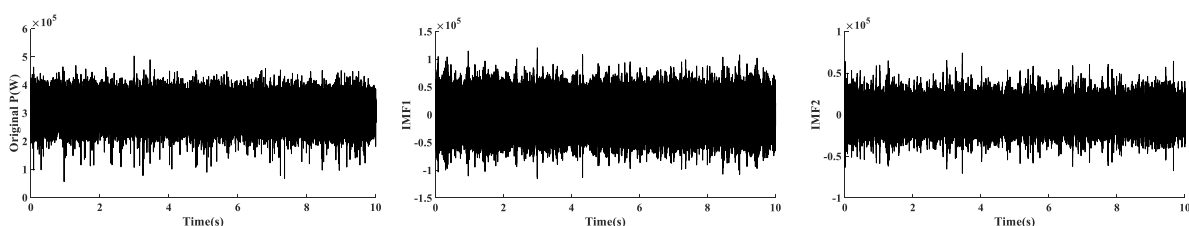
Table 1. Energy ratio and power volatility (%)

IMF	1	2	3	4	5	6	7	8	9	10	11	12	13
Energy ratio	58.51	12.33	13.69	8.88	3.30	1.68	0.86	0.36	0.17	0.10	0.06	0.02	0.03

According to the expression of vibration function (11) we can obtain A, λ, w and θ_0 by fitting instantaneous amplitude and phase of IMF1~IMF7, as shown in table 2. And the approximate frequencies are 48.46 Hz, 21.67 Hz, 14.32 Hz, 6.01 Hz, 2.01 Hz, 1.62 Hz and 0.37 Hz. Compared with the results of small signal analysis on the same wind turbine, we can find that 21.67 Hz is the frequency of SSR, 14.32 Hz, 2.01 Hz and 1.62 Hz are the frequencies of SSO, 6.01 Hz is the frequency of SSCI, 0.37 Hz is the frequency of LFO. Also, based on the initial amplitude we can conclude that the influence of SSCI is greater than SSR and LOF. And SSO is common in the output power. Additionally, ζ of each IMF can be calculated by (14).

Table 2. Characteristic parameters

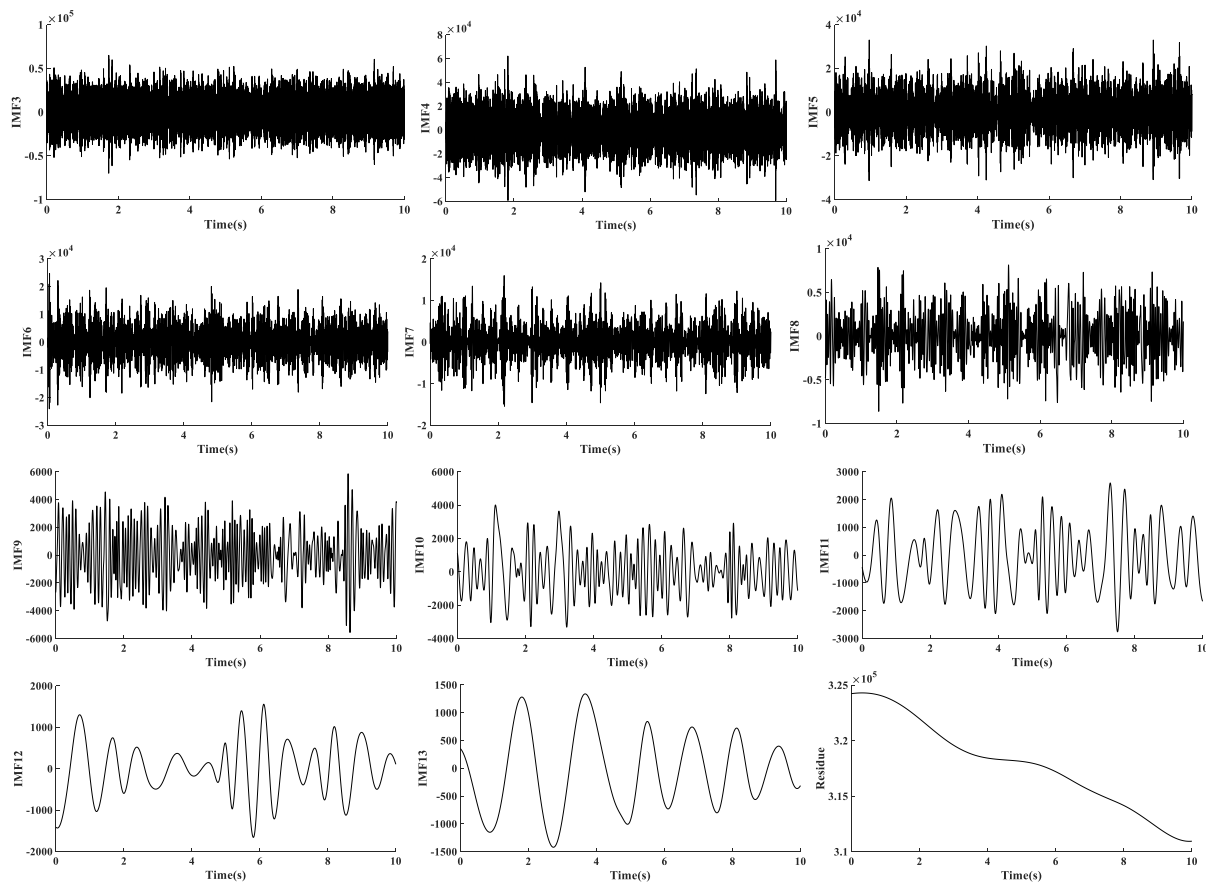| IMF	1	2	3	4	5	6	7
A	3.999e4	1.693e3	1.833e4	1.474e4	8.418e3	6.275e3	4.297e3
λ	0.0046	0.0015	0.0026	0.0082	0.0029	0.0062	0.0018
w	304.313	136.096	89.938	37.736	12.623	10.167	2.333
θ_0	-0.0034	0.0036	0.0079	0.0064	-0.0011	0.0006	0.0069
ζ	0.212	0.672	0.034	0.721	0.344	0.362	0.325

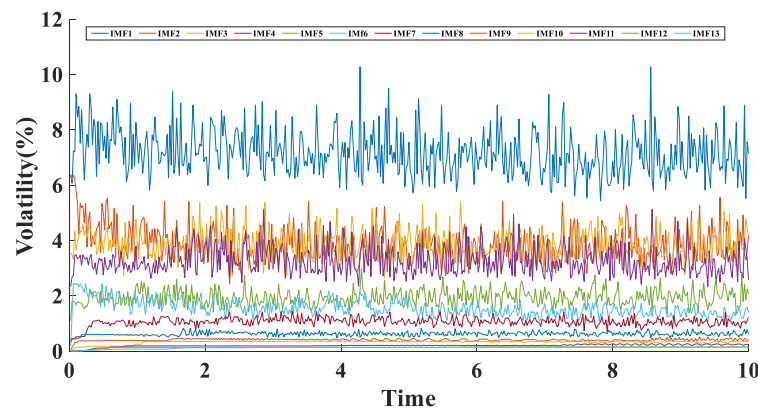**Figure 3.** Original signal, IMFs and residue of wind power

Figure 4. Power volatility of IMFs

5. Conclusions

This paper effectively analyses turbine-grid interaction in output power of wind turbine with methods based on HHT. And with the results of actual case, the following conclusions can be drawn:

- Low frequency noise can be removed from the output power of wind turbine according to energy ratios and power volatilities after the EMD process.
- In output power of wind turbine, SSR, SSO, SSCI and LOF can be find clearly, and they all have impact on the output power.
- Specifically, the influences of SSCI and SSO are severer than SSR and LOF. And SSO with the frequency of 14.32 Hz has a stronger effect than 2.01 Hz and 1.62 Hz.

Since the ability of HHT drop off rapidly when it is used to process the signal containing components with close frequencies, results obtained by methods based on HHT always have some error. Thus, we

can improve the skill of frequency resolution of our methods to polish up the case results and further study the turbine-grid interaction.

6. References

[1]   A. S. Bubshait, A. Mortezaei, M. Simoes, et al. Power Quality Enhancement for a Grid Connected Wind Turbine Energy System [J]. IEEE Transactions on Industry Applications, 2017, PP (99):1-1.

[2]   B. Badrzadeh, M. Sahni, Y. Zhou, et al. General methodology for analysis of sub-synchronous interaction in wind power plants [C]// Power and Energy Society General Meeting. IEEE, 2013:1858 - 1869.

[3]   H. Liu, X. Xie, J. He, et al. Subsynchronous Interaction between Direct-Drive PMSG Based Wind Farms and Weak AC Networks [J]. IEEE Transactions on Power Systems, 2017, PP (99):1-1.

[4]   T. M. Cesar, S. P. Pimentel, E. G. Marra, et al. Wavelet Transform analysis for grid-connected photovoltaic systems [C]// International Conference on Clean Electrical Power. 2017:1-6.

[5]   M. Ghafouri, U. Karaagac, H. Karimi, et al. An LQR Controller for Damping of Subsynchronous Interaction in DFIG-Based Wind Farms [J]. IEEE Trans. on Power Systems, 2017, PP (99):1-1.

[6]   C. Li, W. Zhang, R. Liu. Forced low frequency oscillation of wind-integrated power systems [C]// Innovative Smart Grid Technologies Conference. IEEE, 2016:1-5.

[7]   H. Liu, X. Xie, J. He, et al. Subsynchronous Interaction between Direct-Drive PMSG Based Wind Farms and Weak AC Networks [J]. IEEE Transactions on Power Systems, 2017, PP (99):1-1.

[8]   L. Peretti, M. Pathmanathan, O. I. U. Haq, et al. Robust harmonic detection, classification and compensation method for electric drives based on the sparse fast Fourier transform and the Mahalanobis distance [J]. Iet Electric Power Applications, 2017, 11(7):1177-1186.

[9]   Z. L. Zhang , X. Cheng, Z. Y. Lu, et al. SOC Estimation of Lithium-ion Batteries with AEKF and Wavelet Transform Matrix [J]. IEEE Transactions on Power Electronics, 2016, PP (99):1-1.

[10]   A. Gururani, S. R. Mohanty, J. C. Mohanta. Microgrid protection using Hilbert–Huang transform based-differential scheme [J]. Iet Generation Transmission & Distribution, 2016, 10 (15):3707-3716.

[11]   Q. Liu, Y. Mitani. Application of HHT for oscillation mode analysis in power system based on PMU[C]// International Conference on Electric Power and Energy Conversion Systems. IEEE, 2012:1-4.

[12]   M. J. Afroni, D. Sutanto, D. Stirling, Analysis of Nonstationary Power-Quality Waveforms Using Iterative Hilbert Huang Transform and SAX Algorithm [J]. IEEE Transactions on Power Delivery, 2013, 28(4):2134-2144.